Advanced Powder Technology 26 (2015) 698–704

Contents lists available at ScienceDirect

Advanced Powder Technology

journal homepage: www.elsevier.com/locate/apt

Original Research Paper

Numerical particle-based analysis of the effects responsible for acoustic particle agglomeration

D. Markauskas *, R. Kačianauskas, A. Maknickas

Vilnius Gediminas Technical University, Vilnius, Lithuania

ARTICLE INFO

Article history:
Received 24 September 2014
Received in revised form 9 December 2014
Accepted 11 December 2014
Available online 24 December 2014

Keywords:
Acoustic agglomeration
Numerical modelling
Discrete element method
Aerosols

ABSTRACT

Numerical particle-based modelling of aerosol particles in an acoustic field is performed, and the influence of the effects, including orthokinetic collision, an acoustic wake effect and mutual radiation pressure effect, responsible for the particle agglomeration is analyzed. The standard discrete element method is modified to take into account the drag force of the gas obtained using Oseen's solution and the mutual radiation pressure force. Numerical modelling of the agglomeration of two identical particles in a strong acoustic field is performed, and the results are compared with the available analytical solution and the data obtained in the experiments described in the literature. Finally, the simulation of a 2D polydispersed particle system at various sound frequencies is performed. The obtained results show that the major agglomeration mechanism is the acoustic wake effect, while orthokinetic collision plays an insignificant role.

1. Introduction

Acoustic agglomeration of dispersed aerosol particles is a process when intense sound waves produce relative motions and collisions between the initial small particles sequentially forming larger particles. Larger particles can be more easily caught using conventional particle filtering devices, and, therefore, acoustic agglomeration is used to significantly enhance the removal rate of the micron size particles [1–3].

The process of acoustic agglomeration is governed by various particle–fluid and particle–particle interactions, and several approaches to acoustic agglomeration have been developed. Theoretical aspects of various agglomeration mechanisms are discussed in [4–7]. Orthokinetic interactions refer to the agglomeration due to direct collisions between particles that are entrained at different velocities in the oscillatory motion of the sound field. The particles of various sizes are entrained differently by the motion of the medium because of the differences in particle inertia. The earlier investigations into orthokinetic collisions date back to the contribution of Mednikov [8]. The important contribution of Dong et al. [9], relating to separate and combined effects of orthokinetic collision, may be also mentioned. Nevertheless, the orthokinetic collision mechanism is able to model particle collisions occurring due to different particle entrainments, but it does not explain the agglomeration of particles of the same or similar size.

Aerosol particles not only interact with the ambient gas, but the interaction between the particles in the gas can be observed. According to the Oseen's solution, an asymmetric flow field is formed around the moving particle. If two particles are in the line with the flow field, then, the drag reduction is less significant for the leading particle, and, as a result, the 'tail' particle moves at an accelerated speed towards the leading one [10]. This hydrodynamic interaction is called "acoustic wake effect" (AWE) [4]. The significance of this effect for the agglomeration of particles was studied in [4,11,6,9,12] by using the analytical and numerical methods and was experimentally verified in [13–15].

Two nearby particles exert forces on each other because their scattered waves nonlinearly interact with the incident acoustic wave. This is known as "mutual radiation pressure effect" (MRPE), the significance of which is pointed out by Gonzalez and Gallego-Jurez [15]. The analytical solution for MRPE force was derived by Song [16,5]. While the experimental and numerical results in [17,13] fail to provide the direct evidence to support the Song's hypothesis of scattering interaction as an effective refill mechanism of the emptied agglomeration volumes, the authors in [15] suggest that MRPE is behind a repulsion effect observed in combination with the attraction exerted by the AWE.

As noted by Zhang et al. [12], the conclusions drown in the cited works about the role of the agglomeration effects do not agree with

* Corresponding author.
E-mail address: darius.markauskas@vgtu.lt (D. Markauskas).

http://dx.doi.org/10.1016/j.apt.2014.12.008

Nomenclature

μ	dynamic viscosity (Pa s)	R	particle radius (m)
ν	kinematic viscosity (m^2/s)	Re	Reynolds number
ω	angular frequency (rad/s)	SPL	sound pressure level (dB)
ρ_g	gas density (kg/m^3)	t	time (s)
ρ_p	particle density (kg/m^3)	U_0	acoustic velocity amplitude (m/s)
AWE	acoustic wake effect	$\mathbf{u}_g$	gas velocity (m/s)
d_p	particle diameter (m)	$\mathbf{u}_{g,ac}$	gas velocity due to acoustic waves (m/s)
$\mathbf{F}_b$	buoyancy force (N)	$\mathbf{u}_{g,pv}$	perturbation gas velocity (m/s)
$\mathbf{F}_d$	drag force (N)	$\mathbf{u}_p$	particle velocity (m/s)
$\mathbf{F}_g$	gravity force (N)	V_p	particle volume (m^3)
$\mathbf{F}_{MRPE}$	mutual radiation pressure effect force (N)	$\ddot{\mathbf{x}}$	particle acceleration (m/s^2)
$\mathbf{g}$	acceleration of gravity (m/s^2)		
m	mass of the particle (kg)		
MRPE	mutual radiation pressure effect		

each other and, sometimes, even contradict one another. Therefore, a more comprehensive study of the effects responsible for acoustic particle agglomeration is still needed.

In the past, the particle agglomeration was numerically modelled by many researchers (e.g. [8,5,4,18,12]). The well-known Smoluchowski equation can be used to solve the discrete particle or cluster dynamic equation [16]. As an alternative method for the simulation of acoustic agglomeration, the direct simulation Monte Carlo method was applied by Sheng and Shen [18].

Aerosol is particulate medium, therefore, the particle-based approach is a natural numerical technique, which could be applied to its simulation [19]. The development of the discrete element method (DEM) for aerosol particles follows formally the conventional path, and is focused on the evaluation of all available particle forces, including binary interactions with the neighbouring partners, particle–fluid interaction and the external field induced forces. A detailed classification of particle forces occurring in fluid may be found in the review papers [20,21]. Concerning the acoustics induced forces, the reviews of [15,22–24] may be mentioned.

In the present work, the DEM methodology was adopted for simulating acoustic agglomeration of aerosol particles, and our in-house DEM code [25,26] was changed for simulation purposes. In Section 2, the methodology and basic relations of the particle interactions applied to the dynamic behaviour of aerosols is described. In Sections 3 and 4, the obtained numerical results are presented.

2. A theoretical model

The model presented below follows the DEM methodology. Three mechanisms used by other authors and potentially responsible for the acoustic agglomeration are described and incorporated into DEM.

The motion of each aerosol particle is governed by the Newton's Second law:

$$m\ddot{\mathbf{x}}_p = \mathbf{F}_d + \mathbf{F}_b + \mathbf{F}_g + \mathbf{F}_{MRPE}, \tag{1}$$

where $\mathbf{F}_d$ is the drag force of gas, $\mathbf{F}_b = V_p\rho_g\mathbf{g}$ is the buoyancy force, V_p is the volume of the particle, $\mathbf{F}_g = m\mathbf{g}$ is the gravity force. The drag force can be established in the Oseen regime [27] by

$$\mathbf{F}_d = 6\pi\mu R\left(1+\frac{3}{16}\mathrm{Re}\right)(\mathbf{u}_g - \mathbf{u}_p), \tag{2}$$

where $\mathrm{Re} = 2R(|\mathbf{u}_g - \mathbf{u}_p|)/\nu$ is the Reynolds number, R is the radius of the particle, μ is dynamic viscosity of the fluid ($\mu = \nu\rho_g$), $\mathbf{u}_g$ and $\mathbf{u}_p$ is gas and particle velocity respectively. The gas velocity $\mathbf{u}_g$ is expressed as

$$\mathbf{u}_g = \mathbf{u}_{g,ac} + \mathbf{u}_{g,pv}, \tag{3}$$

where $\mathbf{u}_{g,pv}$ is the perturbation gas velocity and $\mathbf{u}_{g,ac}$ is the vector of gas velocity due to acoustic motion, whose one component is equal to

$$u_{g,ac} = U_0\sin(\omega t). \tag{4}$$

Note, that the spatial variation of acoustic velocity is neglected in Eq. (4).

Particle collisions due to different particle oscillations in the acoustic field (4) (when $u_{g,pv}$ is neglected in Eq. (3)) is called the orthokinetic collision (OC) mechanism [9]. However, it is clear that this mechanism can cause the agglomeration of different size particles only, while the agglomeration of similar sized particles cannot be explained by it.

The perturbation gas velocity $u_{g,pv}$ is calculated based on the steady Oseen approximation [27]. However the use of Oseen approximation may not be necessarily justified in the theoretically strict meaning. Owing to the nonlinear convection term in Navier–Stokes equation, Oseen approximation for oscillatory flow past a sphere can take a completely different form from that for stationary flow. There are no theoretical bases that the flow pattern of oscillatory flow is similar to that of steady flow. Deeper considerations on this theoretical matter can be found in [28]. In the present work the perturbation gas velocity $u_{g,pv}$ in the polar coordinates is described in the Oseen regime by the equations presented in [29] at the position of particle i generated by particle k (Fig. 1):

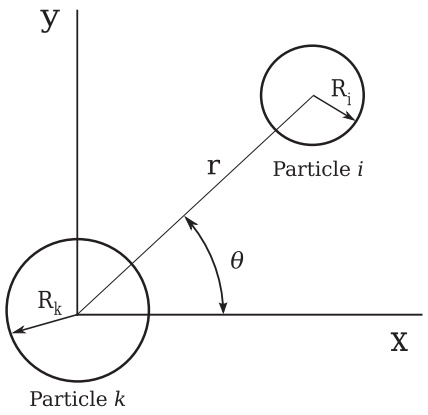

Fig. 1. The calculation scheme of two particles.

$$v_{ik,r} = \frac{A_0}{r^2} - \frac{A_0 e^{\frac{-r(|v_k| - v_k\cos\theta)}{2v}}}{r^2}\left(1 + r\frac{|v_k| + v_k\cos\theta}{2v}\right),$$
$$v_{ik,\theta} = \frac{-A_0 v_k}{2rv}\sin\theta e^{\frac{-r(|v_k| - v_k\cos\theta)}{2v}}, \quad (5)$$

where $A_0 = \frac{3}{2}vR_k\left(1 + \frac{3R_k}{8v}|v_k|\right)$ and $v_k = u_{g,ac} - u_p$ is the relative velocity of the particle. Then, the perturbation gas velocity $u_{g,pv}$ in the Cartesian coordinate system is obtained from Eq. (5) by

$$u_{g,pv,x} = v_{ik,r}\cos\theta - v_{ik,\theta}\sin\theta$$
$$u_{g,pv,y} = v_{ik,r}\sin\theta + v_{ik,\theta}\cos\theta. \quad (6)$$

An illustration of stream lines of the perturbation velocity around the moving spherical particle is shown in Fig. 2. An asymmetric flow pattern is clearly seen on the figure by comparing the stream lines in front and behind the sphere. This asymmetry causes the different reduction of the drag force.

Eqs. (3)–(6) allow us to analyse the influence of the so-called hydrodynamic acoustic wake effect (AWE) [9], where the presence of one particle influences the movement trajectory of another particle.

According to Song [5,16], two nearby particles are not only entrained into the primary acoustic field, but also oscillate with the fluid motion of the scattered wave fields. This is referred to as the mutual radiation pressure effect (MRPE), a hydrodynamic mechanism of interaction taken into account together with the AWE, as suggested in [15].

Danilov and Mironov [30] used method, by which the hydrodynamic force on one of two interacting particles is calculated by evaluating the total time-average momentum flux of the fluid through a closed surface which encloses that particle. This method is modified by Song [16] to include the effects of the partial entrainment of the particles and the viscous wave scattered from the particles. An average radiation pressure force in the spherical coordinates in one acoustic cycle ([16], p. 115, Eq. 4.36–4.37) is as follows:

$$f_{ki,r} = \frac{3\rho_0 U_i^2}{16\pi}a_1^3 a_2^3\frac{3\cos^2\theta - 1}{r^4}g_{ki,r}(r,\theta),$$
$$f_{ki,\theta} = \frac{3\rho_0 U_i^2}{16\pi}a_1^3 a_2^3\frac{\sin 2\theta}{r^4}g_{ki,\theta}(r), \quad (7)$$

where $g_{ki,r}$ and $g_{ki,\theta}$ are defined as the hydrodynamic interaction functions that show a very complex dependence on r and θ [16]. The mutual radiation pressure force $\mathbf{F}_{MRPE}$ is obtained by transforming $f_{ki,r}$ and $f_{ki,\theta}$ into the Cartesian coordinate system.

In Eq. (7), $f_{ki,r}$ and $f_{ki,\theta}$ are inversely proportional to the fourth power of the radial distance r between two interacting particles. Therefore, MRPE may be relevant only to the particle collision processes if the separation distance between the particles is small.

The equation of motion (1) should be solved for every particle in the system. This is achieved by explicit time integration using the velocity Verlet scheme with fixed time step [31]. To achieve accurate results, a small time step should be used in numerical simulations. On the other hand, the small time step increases the computational time required, which is important for simulations of larger particle systems. Therefore, the time step not larger than 1/250 of the period of the sound wave was chosen for simulations, when several numerical tests had been performed.

The contact between particles is checked at each time step during the simulation. If the contact is found, the coagulation of particles is assumed, and two particles are merged into one bigger spherical particle using the relations:

$$V_{p,new} = V_{pi} + V_{pk},$$
$$\mathbf{u}_{p,new} = \frac{\mathbf{u}_{pi}m_{pi} + \mathbf{u}_{pk}m_{pk}}{m_{pi} + m_{pk}}, \quad (8)$$
$$\mathbf{x}_{p,new} = \frac{\mathbf{x}_{pi}m_{pi} + \mathbf{x}_{pk}m_{pk}}{m_{pi} + m_{pk}},$$

where subscripts pi and pk denote the particles in contact, while subscript p,new is for the merged particle. V, m and $\mathbf{x}$ are the volume, the mass and the coordinates of the respective particle.

The presented theoretical model (Eqs. (2)–(8)) for calculating the motion of particles in the acoustic field is similar to the model used in the standard discrete element method (e.g. [32,33]). However, (a) no contact forces are calculated there and (b) long-range forces (F_d, F_{MRPE}) should be calculated in contrast to the standard DEM. In Sections 3 and 4, this model is used for the numerical analysis of the particle motion in the acoustic field.

3. The numerical tests

3.1. A falling particle

The theoretical model presented in the previous section and implemented into the computational program was tested for a simple case of a falling particle without the acoustic field. The terminal velocity of falling spherical particle was calculated numerically and compared with the analytical result obtained from Stokes equation [34]. The results for different particle sizes (particle diameter varies between 1 μm and 24 μm) are presented in Fig. 3. This comparison shows very good agreement between the numerical simulation and the analytical results when no acoustic field is applied and proves the validity of the developed computational algorithm for calculating the movement of particles when no acoustic field is applied.

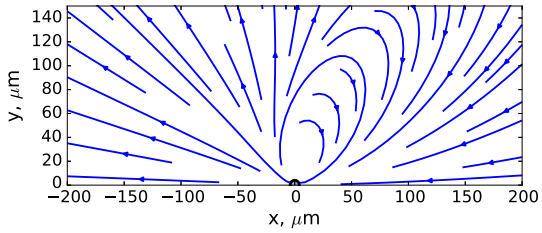

Fig. 2. Streamlines of the perturbation velocity around a spherical particle moving to the left in a stagnant fluid ($d_p = 8$ μm, $v_{k,x} = -1$ m/s, Re = 0.52).

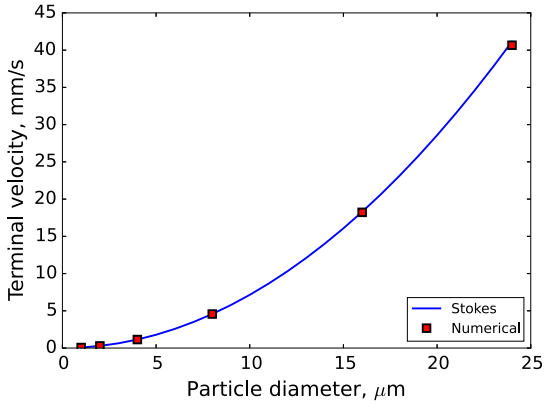

Fig. 3. Terminal velocity as a function of particle diameter: line represents analytical prediction using Stokes solution ($\rho_p = 2400$ kg/m^3).

3.2. The agglomeration of two particles: the comparison with the analytical solution

The numerical solution of the convergence velocity of two particles u_{12} was compared to the analytical solution derived by Dianov et al. [10]:

$$u_{12} = \frac{3U_0}{2\pi r}(R_1 l_1 + R_2 l_2), \tag{9}$$

where l_1 and l_2 are the functions of ρ_p, ρ_g, ω and R.

Two particles with equal diameters ($d_1 = d_2 = 8$ μm, $\rho_p = 1000$ kg/m^3) were placed at the initial distance of 200 μm and subjected to the action of the acoustic field ($U_0 = 2$ m/s, SPL 149.3 dB). The air properties at 20 °C were used ($\mu = 18.3$ μPa s, $\rho_g = 1.2$ kg/m^3). If no perturbation velocity $u_{g.pv}$ (Eq. (3)) is calculated, then, the particles just oscillate around the initial position, not approaching each other. However, when $u_{g.pv}$ is calculated, then, two particles approach each other and, eventually, merge into one bigger particle.

The results of simulation, together with the curve from the analytical solution, are presented in Fig. 4. Since the particles in the numerical simulation have zero initial velocity, it requires several acoustic cycles until the particles are entrained. As can be seen, relative particle velocity u_{12} in the numerical solution varies with time, but the mean values of u_{12} are very close to analytical results, when two particles are far apart. When two particles are approaching each other, the difference between the analytical and numerical solutions starts to appear at about 100 μm and increases rapidly, when two particles continue to approach. This difference can be explained by the fact that, during the derivation of Eq. (9), some terms of the equation, which are not relevant when particles are far apart, are dropped.

3.3. The agglomeration of two particles: comparison with the experimental data

The comparison between the results of the numerical simulation and experimental results reported by Gonzalez and Gallego-Jurez [15] is presented below. In the experiments [15], small glass spheres (the diameter $d_p = 8$ μm) were subjected to the action of the horizontal acoustic field ($U_0 = 0.44$ m/s, SPL 136.1 dB) and the process of agglomeration was filmed. The results of the comparison are presented in Figs. 5 and 6. Fig. 5 shows the trajectories of the particles, initially aligned along the acoustic axis, moving in the acoustic field of 900 Hz at the initial distance between the centres of the particles equal to 207 μm. The entrainment factor was obtained to be equal to 0.357 in the numerical experiments, while the reported value in the real experiment was about 0.35. Fig. 5(a) presents the results obtained without taking into account the MRPE force F_{MRPE} (Eq. (1)), while in Fig. 5(b), the results are obtained with the MRPE force. As can be seen from the figures, the MRPE force changes the way how two particles approach each other. When the distance between the particles is smaller, the particles in Fig. 5(a) start approaching each other more quickly and form a parabola-like trajectory. This shape of the trajectory is similar to that measured in the real experiment. However, the trajectories of the particles are of different shape, when the MRPE force is added (Fig. 5(b)). The measured agglomeration time is equal to 26 ms in the case, when the MRPE force is not applied, which is in quite good agreement with the approximate value 30 ms obtained in the real experiment. The measured agglomeration time is equal to 84 ms for the case with the MRPE force applied. Vertical particle velocity of 7.2 mm/s can be calculated from the picture presented in [15] for the case of the acoustic frequency $f = 900$ Hz. However, a smaller value of vertical velocity 4.5 mm/s, was obtained in the numerical tests, while the analytical terminal velocity from the Stokes equation is equal to 4.6 mm/s.

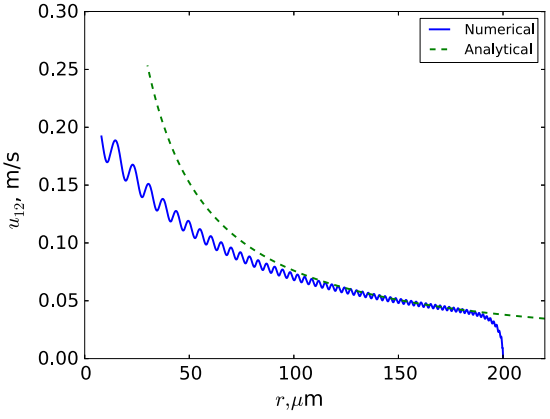

Fig. 4. Comparison with the Dianov's solution.

Fig. 6 shows the trajectories of particles, moving in the acoustic field of 3000 Hz at the initial horizontal distance between the centres of two particles equal to 190 μm and an angle between the particles equal to 19° with respect to the axis of the horizontal acoustic field. The entrainment factor was obtained to be 0.11 in the numerical experiments, while the reported value in the real experiment was equal to 0.08. Similar to the previous case, the MRPE force changes the way how two particles approach each other. The calculated agglomeration time is equal to 23 ms in the case without applying the MRPE force, which is similar to the measured value of 20 ms in the real experiment. The numerically obtained agglomeration time is equal to 48 ms for the case with the applied MRPE force. Vertical particle velocity about 36 mm/s is calculated from the picture presented in [15] for the case of the acoustic frequency $f = 3000$ Hz and the sound velocity amplitude $U_0 = 0.44$ m/s. However, the values for the numerical and the analytical terminal velocity remain unchanged ($v_{term,num} = 4.5$ mm/s, $v_{term,anal} = 4.6$ mm/s) because the horizontal acoustic field does not influence the vertical movement of the particle in the applied model.

First, the presented results allow us to conclude that the main mechanism responsible for the particle agglomeration is AWE, while the known solution for the MRPE demonstrates the non-physical character of particle agglomeration. Second, it seems that the horizontal acoustic field influences the vertical particle velocity, however, the presented model cannot take into account this influence.

The comparison between the numerical and experimental results demonstrates that considerable differences still exist. Consequently, the more detailed numerical analysis and more accurate experiments are required in further investigations.

4. Simulation of 2D particle system

In this section, the simulation of the particle system in the horizontal acoustic field is performed. Forces, acting on each particle, are the drag force F_d, the buoyancy force F_b and the gravity force F_g (Eq. (1)). Here, F_d is influenced by the perturbation gas velocity $u_{g.pv}$ (Eq. (3)), which means that AWE is taken into account. However, F_{MPRE} has not been calculated for the particles in this numerical analysis, because F_{MPRE} caused doubtful agglomeration patterns in Section 3.3. It should be noted, that the Cunningham correction factor for the drag force [35] may be important for such small particles as used in the simulations, however, it was not applied in the presented work.

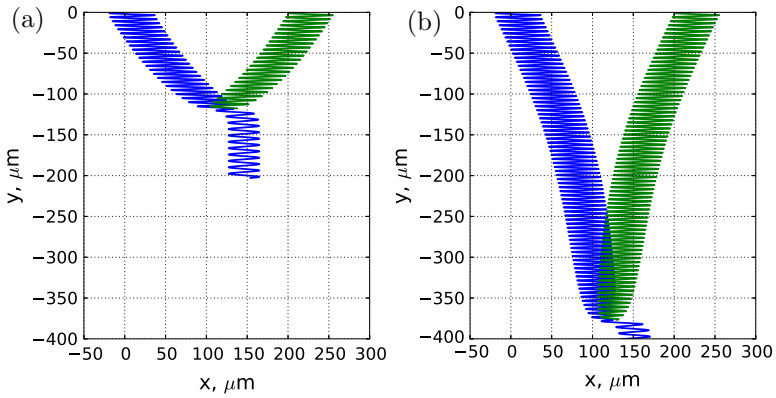

Fig. 5. Agglomeration of two particles (f = 900 Hz, U_0 = 0.44 m/s): (a) without applying the MRPE force; (b) with the MRPE force applied.

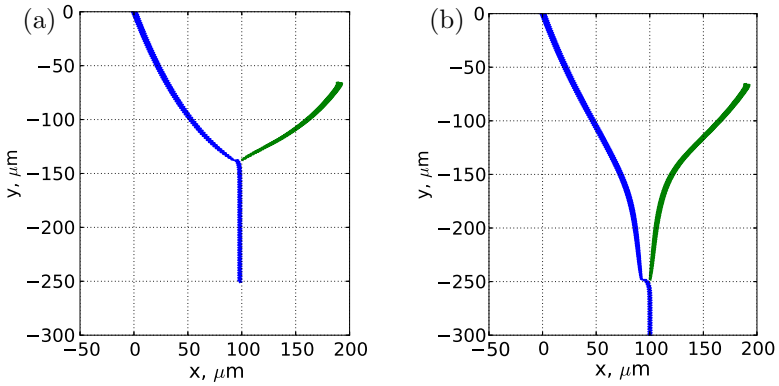

Fig. 6. Agglomeration of two particles (f = 3000 Hz, U_0 = 0.44 m/s): (a) without applying the MRPE force; (b) with the MRPE force applied.

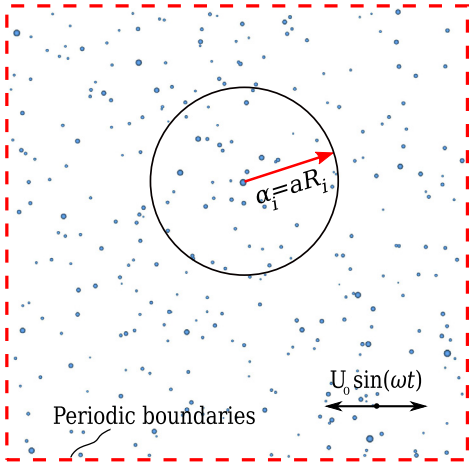

Fig. 7. 2D simulation domain.

For the sake of simplicity, we limited our research to a two-dimensional case. The real space with small particles, where the acoustic agglomeration takes place (e.g. some sort of a filtering system), is usually very large and has a lot of particles. Modelling of this system would be impossible, therefore, only a small part of the whole system was selected and used in the simulations. A small simulation domain of this type is shown in Fig. 7. Since it is only a cut, periodic boundary conditions are used for all four sides of the domain [36]. In periodic boundary conditions, the simulation box is replicated throughout space to form an infinite lattice. When a particle moves in the simulation box, the motion of its periodic image in every one of the other boxes is the same. When the particle passes through one side of the simulation box, it re-appears on the opposite side with the same velocity. Each particle interacts with the other surrounding particles on the simulation and replicated boxes. The minimum image convention is used, by which the particle may interact only with the particles whose centres lie within distance no larger than half of the width of the simulation box.

The particle size distribution used in the current research is the same as that used in the experiments reported in [37]. At the beginning of simulation, the particles are randomly distributed in the simulation domain and the horizontal acoustic field is applied. Simulation parameters are presented in Table 1. An example of initial particle distribution is presented in Fig. 7. Note, that the diameters of the particles are multiplied 10 times in Fig. 7 just for visualization purposes (it would be impossible to see the particles of real size which were used in the simulations).

Table 1
Simulation parameters of the 2D particle system.

Parameter	Value
Particle size distribution	log-normal
Geometric mean particle diameter	0.8 μm
Geometric standard deviation	1.3
Initial number of particles	300/1 mm^2
Density of particles, ρ_p	1118 kg/m^3
Dynamic gas viscosity, μ	$18.3 \cdot 10^{-6}$ Pa s
Acoustic amplitude, U_0	1.0 m/s
Sound pressure level, SPL	143.3 dB

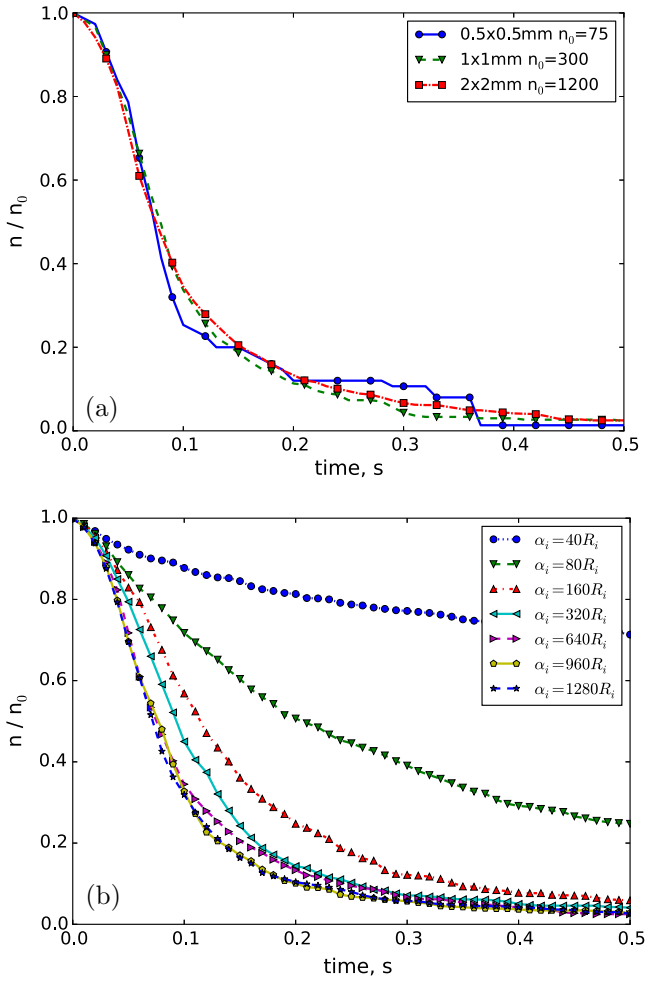

Fig. 8. The analysis of the numerical parameters: (a) the influence of size of the simulation domain; (b) the influence of the radius α_i.

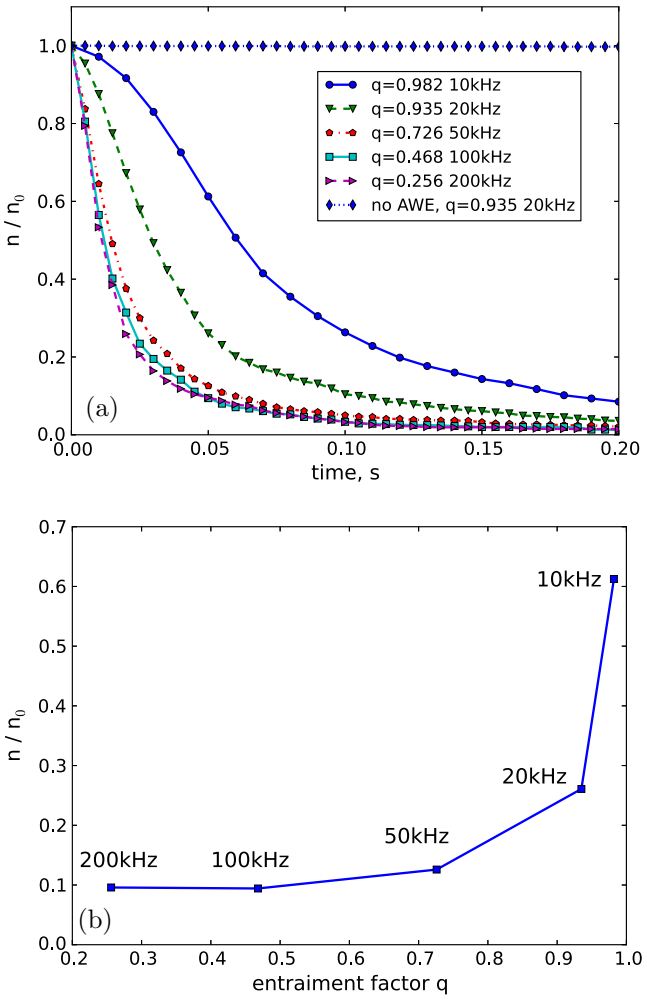

Fig. 9. The influence of agglomeration velocity: (a) the normalized number of particles n/n_0 vs time of impact; (b) the dependence of the normalized number of particles n/n_0 on the entrainment factor calculated for a particle with the mean diameter at $t = 0.05$ s.

First, the analysis was carried out to answer the question, what minimum size of simulation domain can be used. Modelling using 0.5×0.5 mm, 1.0×1.0 mm and 2.0×2.0 mm simulation domains was performed. The results obtained are presented in Fig. 8(a). In this figure, the change of the normalized number of particles, n/n_0, during the simulations is demonstrated. Here, n is the current number of particles and n_0 is the initial number of particles. It can be seen, that if 0.5×0.5 mm domain is used, the relative number of particles changes more stepwise. Only when the simulation domain of 2.0×2.0 mm is used, the agglomeration curve remains smooth. Therefore, the simulation domain of this size is used further.

In general, every particle in the domain influences the movement of all other particles because of AWE (see Eqs. (3)–(6)). However, if the distance between the two particles is large, the influence is very small (see Eq. (5)). Therefore, the calculation of forces acting on a particle is limited to the surrounding particles in the radius $\alpha_i = aR_i$ from the particle itself (Fig. 7), where R_i is the particle radius, while the parameter a is predefined at the start of simulation. It means that all particles, which are in the radius α_i around the particle i, influence the motion of the particle through the calculated perturbation gas velocity $u_{g.pv}$. A series of simulations using the various values of the parameter a is performed and the results are presented in Fig. 8(b). It can be seen, that the agglomeration with the radius $\alpha_i = 40R_i$ is very slow. Agglomeration velocity increases, when more particles are taken into account (a larger α_i is used) for calculating the forces. However, when α_i reaches approximately $960R_i$, the change of α_i does not make any significant influence. Therefore, $\alpha_i = 960R_i$ has been selected for further tests.

The modelling of the agglomeration of a particle system is performed. The influence of different agglomeration effects and different acoustic frequencies in the range of 10–200 kHz is analyzed. In the studied model, the spatial variation of acoustic velocity is neglected (see Eq. (4)). Therefore, presented simulations does not treat the standing wave case with short wave length, where particles may gather in the nodes or antinodes of acoustic pressure. The results are presented in Fig. 9. Fig. 9(b) shows how the normalized number of particles depends on the entrainment factor, which is calculated for the mean particle diameter of the initial particle system ($t = 0$ s). Fig. 9(a) demonstrates how the normalized number of particles changes in time at various frequencies, when AWE is calculated.

As can be seen, the agglomeration process is very fast: 0.2 s is sufficient to reduce the number of particles by factor 10 and more. However, the influence of the acoustic field depends on frequency. The agglomeration in the 10 kHz acoustic field is the slowest process. An increase in the acoustic frequency from 10 kHz to 20 kHz determines how fast the agglomeration takes place (see Fig. 9(b)).

However, when the acoustic frequency increases from 50 kHz to 200 kHz, no great difference can be observed.

When no AWE is calculated (the last line on the legend Fig. 9(a)), only very few particle agglomerations occur and, therefore, this line remains almost horizontal at $n/n_0 = 1.0$. This shows, that the orthokinetic collision effect (OCE) produces very small influence on the acoustic agglomeration. The comparisons with the experimental data presented in Section 3.3 allow us to assume, that the theoretical model cannot adequately describe the vertical particle velocity in the acoustic field. The expected increase in the vertical particle velocity can cause some changes in the agglomeration of particles due to the OCE. However, this possible increase in the number of agglomerations cannot significantly change the influence of OCE.

5. Conclusions

In the current research, the numerical analysis of three agglomeration effects, i.e. orthokinetic collision, acoustic wake effect and mutual radiation pressure effect, was presented. The numerical method, based on the well-known discrete element method, was used for the analysis. Based on the performed numerical analysis, the following conclusions can be drawn:

- Modelling of two identical particles has shown that the main mechanism responsible for acoustic agglomeration is the acoustic wake effect.
- The known solution for mutual radiation pressure effect has shown non-physical behaviour of two particles in the process of agglomeration.
- Quite good agreement between numerical and experimental results relating to the entrainment factor and the agglomeration time could be observed. However, the performed numerical modelling and the experiments have shown significant differences between the vertical particle velocities in the acoustic field, especially, at higher frequencies (for lower entrainment factors). Real experiments demonstrate the influence of the vertical particle velocity on the acoustic field. However, the presented theoretical model cannot take into account this influence.
- Modelling of the 2D system of polydispersed particles demonstrated that the orthokinetic mechanism plays an insignificant role in the agglomeration of particles in the system, while the acoustic wake effect is a major agglomeration mechanism responsible for particle agglomeration in the case of travelling acoustic waves.

Acknowledgment

This research was funded by the Project of Scientific Groups (Research Council of Lithuania), Contract No. MIP-072/2013.

References

[1] J. Gallego-Juárez, E. de Sarabia, G. Rodríguez-Corral, T. Hoffman, J. Gálvez-Moraleda, J. Rodríguez-Maroto, et al., Application of acoustic agglomeration to reduce fine particle emissions from coal combustion plants, Environ. Sci. Technol. 33 (1999) 3843–3852.
[2] J. Liu, G. Zhang, J. Zhou, J. Wang, W. Zhao, K. Cen, Experimental study of acoustic agglomeration of coal-fired fly ash particles at low frequencies, Powder Technol. 193 (1) (2009) 20–25.
[3] V. Vekteris, V. Strishka, D. Ozarovskis, V. Mokshin, Experimental investigation of processes in acoustic cyclone separator, Adv. Powder Technol. 25 (3) (2014) 1118–1123.
[4] R. Tiwary, G. Reethof, Hydrodynamic interaction of spherical aerosol particles in a high intensity acoustic field, J. Sound Vib. 108 (1) (1986) 33–49.
[5] L. Song, G.H. Koopmann, T.L. Hoffmann, An improved theoretical model of acoustic agglomeration, J. Vib. Acoust. 116 (2) (1994) 208–214.
[6] I. González-Gómez, T.L. Hoffmann, J.A. Gallego-Juárez, Theory and calculation of sound induced particle interactions of viscous origin, Acta Acust. United Acust. 86 (5) (2000) 784–797.
[7] J. Liu, J. Wang, G. Zhang, J. Zhou, K. Cen, Frequency comparative study of coal-fired fly ash acoustic agglomeration, J. Environ. Sci. 23 (11) (2011) 1845–1851.
[8] E. Mednikov, Acoustic Coagulation and Precipitation of Aerosols, Consultants Bureau, 1965.
[9] S. Dong, B. Lipkens, T. Cameron, The effects of orthokinetic collision, acoustic wake, and gravity on acoustic agglomeration of polydisperse aerosols, J. Aerosol Sci. 37 (4) (2006) 540–553.
[10] D.B. Dianov, A.A. Podol'skii, V. Turubaro, Calculation of the hydrodynamic interaction of aerosol particles in a sound field under oseen flow conditions, Sov. Phys. Acoust. 13 (1968) 367–374.
[11] B. Schetter, J. Funcke, Agglomeration der dispersen phase von aerosolen durch starke schallfelder, Forsch. Ingenieurwes. A 56 (5) (1990) 148–149.
[12] G.X. Zhang, J.Z. Liu, J. Wang, J.H. Zhou, K.F. Cen, Numerical simulation of acoustic wake effect in acoustic agglomeration under oseen flow condition, Chin. Sci. Bull. 57 (19) (2012) 2404–2412.
[13] T.L. Hoffmann, G.H. Koopmann, Visualization of acoustic particle interaction and agglomeration: theory evaluation, J. Acoust. Soc. Am. 101 (6) (1997) 3421–3429.
[14] I. González, T.L. Hoffmann, J.A. Gallego, Precize measurements of particle entrainment in a standing-wave acoustic field between 20 and 3500 Hz, J. Aerosol Sci. 31 (12) (2000) 1461–1468.
[15] I. Gonzalez, J. Gallego-Jurez, The influence of entrainment on acoustically induced interactions between aerosol particles – an experimental study, J. Aerosol Sci. 34 (2003) 1611–1631.
[16] L. Song, Modeling of Acoustic Agglomeration of Fine Aerosol Particles, Ph.D. Thesis, The Pennsylvania State University, 1990.
[17] T.L. Hoffmann, G.H. Koopmann, Visualization of acoustic particle interaction and agglomeration: theory and experiments, J. Acoust. Soc. Am. 99 (4) (1996) 2130–2141.
[18] C. Sheng, X. Shen, Modelling of acoustic agglomeration processes using the direct simulation monte carlo method, J. Aerosol Sci. 37 (1) (2006) 16–36.
[19] J. Marshall, Discrete-element modeling of particulate aerosol flows, J. Comput. Phys. 228 (5) (2009) 1541–1561.
[20] H. Zhu, Z. Zhou, R. Yang, A. Yu, Discrete particle simulation of particulate systems: theoretical developments, Chem. Eng. Sci. 62 (13) (2007) 3378–3396.
[21] N. Deen, M.V.S. Annaland, M.V. der Hoef, J. Kuipers, Review of discrete particle modeling of fluidized beds, Chem. Eng. Sci. 62 (1–2) (2007) 28–44.
[22] L. Xiang, W. Shuyan, L. Huilin, L. Goudong, C. Juhui, L. Yikun, Numerical simulation of particle motion in vibrated fluidized beds, Powder Technol. 197 (1–2) (2010) 25–35.
[23] S. Li, J.S. Marshall, G. Liu, Q. Yao, Adhesive particulate flow: the discrete-element method and its application in energy and environmental engineering, Prog. Energy Combust. Sci. 37 (6) (2011) 633–668.
[24] W. Shuai, L. Xiang, L. Huilin, L. Guodong, W. Jiaxing, X. Pengfei, Simulation of cohesive particle motion in a sound-assisted fluidized bed, Powder Technol. 207 (1–3) (2011) 65–77.
[25] D. Markauskas, R. Kačianauskas, Investigation of rice grain flow by multi-sphere particle model with rolling resistance, Granular Matter 13 (2) (2011) 143–148.
[26] R. Kačianauskas, A. Maknickas, A. Kačeniauskas, D. Markauskas, R. Balevičius, Parallel discrete element simulation of poly-dispersed granular material, Adv. Eng. Softw. 41 (1) (2010) 52–63 (civil-Comp Special Issue).
[27] C. Oseen, Über die stokessche formel und über eine verawandte aufgabe in der hydrodynamik, Astronomi och Fysik 6 (1910) 29.
[28] Y. Nakajima, T. Sato, Electrostatic collection of submicron particles with the aid of electrostatic agglomeration promoted by particle vibration, Powder Technol. 135–136 (2003) 266–284.
[29] N. Kochin, I. Kibel, Theoretical Hydrodynamics [in Russian] (p. Part 2), Fizmatgiz, Moskow, 1963.
[30] S.D. Danilov, M.A. Mironov, Radiation pressure force acting on a small particle in a sound field, Sov. Phys. Acoust. 30 (1984) 276–279.
[31] F. Fraige, P. Langston, Integration schemes and damping algorithms in distinct element models, Adv. Powder Technol. 15 (2) (2004) 227–245.
[32] R. Balevičius, R. Kačianauskas, Z. Mróz, I. Sielamowicz, Analysis and DEM simulation of granular material flow patterns in hopper models of different shapes, Adv. Powder Technol. 22 (2) (2011) 226–235.
[33] A.-N. Huang, H.-P. Kuo, Developments in the tools for the investigation of mixing in particulate systems – a review, Adv. Powder Technol. 25 (1) (2014) 163–173.
[34] A. Nguyen, H. Stechemesser, G. Zobel, H. Schulze, An improved formula for terminal velocity of rigid spheres, Int. J. Miner. Process. 50 (1–2) (1997) 53–61.
[35] M.L. Eggersdorfer, S.E. Pratsinis, Agglomerates and aggregates of nanoparticles made in the gas phase, Adv. Powder Technol. 25 (1) (2014) 71–90.
[36] M. Allen, D. Tildesley, Computer Simulation of Liquids, Oxford University Press, Oxford, 1987.
[37] P. Capéran, J. Somers, K. Richter, S. Fourcaudot, Acoustic agglomeration of a glycol fog aerosol: Influence of particle concentration and intensity of the sound field at two frequencies, J. Aerosol Sci. 26 (4) (1995) 595–612.